Anal. Chem. **2008,** *80,* 2888−2894

Electrogenerated Chemiluminescence DNA Biosensor Based on Hairpin DNA Probe Labeled with Ruthenium Complex

Jing Zhang, Honglan Qi, Yan Li, Jia Yang, Qiang Gao, and Chengxiao Zhang*

Key Laboratory of Applied Surface and Colloid Chemistry, Ministry of Education, School of Chemistry and Materials Science, Shaanxi Normal University, Xi'an 710062, China

A highly selective electrogenerated chemiluminescence (ECL) biosensor for the detection of target single-strand DNA (ss-DNA) was developed using hairpin DNA as the recognition element and ruthenium complex as the signal-producing compound. The ECL-based DNA biosensor was fabricated by self-assembling the ECL probe of thiolated hairpin DNA tagged with ruthenium complex on the surface of a gold electrode. In the absence of target ss-DNA, the ECL probe immobilized on the surface of the electrode was in the folded configuration in which its termini were held in close proximity to the electrode, and thus a strong ECL signal could be generated. In the presence of target ss-DNA, a stem-loop of the ECL probe on the electrode was converted into a linear double-helix configuration due to hybridization, resulting in the tag moving away from the electrode surface, which in turn decreased the ECL signal. The ECL intensity of the DNA biosensor generated a "switch off" mode, which decreased with an increase of the concentration of target DNA, and a detection limit of 9×10^{-11} M complementary target ss-DNA was achieved. Single mismatched target ss-DNA was effectively discriminated from complementary target ss-DNA. The effect of different loop lengths of the hairpin DNA on the selectivity of the ECL DNA biosensor has been investigated. This work demonstrated that the sensitivity and specificity of an ECL DNA biosensor could be greatly improved using a hairpin DNA species which has an appropriate stem and loop length as the recognition element.

DNA hybridization detection has recently attracted much attention due to its diverse applications including the identification of genetic diseases and disorders and the detection and characterization of viruses, bacteria, and parasites.[1] Wide-scale DNA hybridization testing requires the development of easy-to-use, fast, inexpensive, and miniaturized analytical devices. Traditional methods for the detection of DNA hybridization, such as gel electrophoresis or membrane blots, are slow and labor-intensive. DNA biosensors commonly rely on the immobilization of single-strand DNA (ss-DNA) as probes on a transducer surface to recognize its complementary target ss-DNA sequence and offer a promising alternative for fast, cheap, and simple detection of target DNA.[2] Various DNA biosensors have been established including optical,[3−6] electrochemical,[7,8] electrogenerated chemiluminescence (ECL),[9] quartz-crystal microbalance,[10,11] and surface plasmon resonance techniques.[12] In these DNA biosensors, ECL biosensors are very promising due to the combination of advantages of both electrochemical and chemiluminescent biosensors, such as high sensitivity and ease of control.

In order to improve the sensitivity and specificity, much work has been done in ECL DNA biosensing. These include the employment of a high quantum efficiency ECL label[13−15] and the use of a multilabeling approach.[16−19] Bard et al.[13] reported an ECL method for the determination of anthrax-related specific DNA sequence with a detection limit of 30 pM, by covalently attaching a 23-mer synthetic ss-DNA species with an amino-modified group at the 5′ end position to the Au(111) substrate, which was precoated with a self-assembled thiol monolayer of 3-mercaptopropanoic acid and then hybridizing with a 23-mer target ss-DNA species tagged with tris(2,2′- bipyridyl) ruthenium(II) as an ECL label. Fang et al.[14] developed an ECL detection method for DNA hybridization based on *N*-(4-aminobutyl)-*N*-ethylisoluminol and

* To whom correspondence should be addressed. Tel: 86-29-85303825. Fax: 86-29-85307567. E-mail: cxzhang@snnu.edu.cn.

(1) Hvastkovs, E. G.; Buttry, D. A. *Anal. Chem.* **2007**, *79*, 6922−6926.
(2) Wang, J. *Anal. Chim. Acta* **2002**, *469*, 63−71.
(3) Taton, T. A.; Lu, G.; Mirkin, C. *J. Am. Chem. Soc.* **2001**, *123*, 5164−5165.
(4) Zhao, X.; Tapec-Dytioco, R.; Tan, W. *J. Am. Chem. Soc.* **2003**, *125*, 11474−11475.
(5) Ahn, S.; Walt, D. R. *Anal. Chem.* **2005**, *77*, 5041−5047.
(6) Laitala, V.; Ylikoski, A.; Raussi, H. M.; Ollikka, P.; Hemmilä, I. *Anal. Biochem.* **2007**, *361*,126−131.
(7) Park, S. J.; Taton, T. A.; Mirkin, C. A. *Science*. **2002**, *295*, 1503−1506.
(8) Wang, J.; Musameh, M.; Lin, Y. *J. Am. Chem. Soc.* **2003**, *125*, 2408−2409.
(9) Xu, X. H.; Yang, H. C.; Mallouk, T. E.; Bard, A. J. *J. Am. Chem. Soc.* **1994**, *116*, 8386−8387.
(10) Yamaguchi, S.; Shimomura, T. *Anal. Chem.* **1993**, *65*, 1925−1927.
(11) Su, X. D.; Robelek, R.; Wu, Y. J.; Wang, G. Y.; Knoll, W. *Anal. Chem.* **2004**, *76*, 489−494.
(12) Ito, M.; Nakamura, F.; Baba, A.; Tamada, K.; Ushijima, H.; Lau, K. H. A.; Manna, A.; Knoll, W. *J. Phys. Chem. C* **2007**, *111*, 11653−11662.
(13) Miao, W. J.; Bard, A. J. *Anal. Chem.* **2003**, *75*, 5825−5834.
(14) Yang, M. L.; Liu, C. Z.; Qian, K. J.; He, P. G.; Fang, Y. Z. *Analyst* **2002**, *127*, 1267−1271.
(15) Calvo-Munoz, M. L.; Dupont-Filliard, A.; Billon, M.; Guillerez, S.; Bidan, G.; Marquett, C.; Blum, L. *Bioelectrochemistry* **2005**, *66*, 139−143.
(16) Miao, W. J.; Bard, A. J. *Anal. Chem.* **2004**, *76*, 5379−5386.
(17) Chang, Z.; Zhou, J. G.; Zhao, K.; Zhu, N. G.; He, P. G.; Fang, Y. Z. *Electrochim. Acta* **2006**, *52*, 575.
(18) Wang, H.; Zhang, C. X.; Li, Y.; Qi, H. L. *Anal. Chim. Acta* **2006**, *575*, 205−211.
(19) Li, Y.; Qi, H. L.; Fang, F.; Zhang, C. X. *Talanta* **2007**, *72*, 1704−1709.

10.1021/ac701995g CCC: $40.75
Published on Web 03/14/2008

labeled a 24-mer probe ss-DNA species for the recognition of a 24-mer target ss-DNA sample immobilized on a polypyrrole-modified electrode with a detection limit of 30 pM. Miao et al.[16] presented an ultrasensitive ECL method for the detection of DNA hybridization of a 23-mer ss-DNA target with 23-mer probe ss-DNA utilizing polystyrene microspheres/beads as the carriers of the ECL labels of $Ru(bpy)_3[B(C_6F_5)_4]$, and the integrated ECL intensity was found to be linearly proportional to the target ss-DNA concentration in a range of 1.0 fM to 10 nM with a detection limit of 5.0 fM. Tris(2,2′-bipyridyl) ruthenium(II)-doped silica (a detection limit of 0.1 pM for 24-mer target with 24-mer probe DNA)[17] and gold nanoparticles (a detection limit of 5.0 pM for 12-mer target with 18-mer probe DNA)[18] as well as carbon nanotubes loaded with tris(2,2′-bipyridyl) ruthenium derivative tags (a detection limit of 9.0 f M for 42-mer target with 21-mer probe DNA and 18-mer capture)[19] for the ECL detection of DNA were also reported. These approaches offer a remarkable amplification of single hybridization events. In recent years, our group has also established ECL methods for the detection of DNA hybridization based on nanoparticles as carriers for multilabel ECL probes,[18,19] and the sensitivity of the ECL methods can be significantly improved. However, by this method, the target analyte must be modified with thiols[18] or will need to be labeled with an ECL reagent, and the detection process is tedious due to the use of a sandwich model.[19]

The selectivity of a DNA biosensor is largely dependent on the chemical and physical properties of the recognition elements. Much effort in the design of DNA biosensing has been put forth in the search for such selective molecules. The molecular beacon, first developed by Tyagi and Kramer in 1996,[20] is one of the most important molecules that possess a single-stranded oligonucleotide with a stem-and-loop structure, in which the 5′ and 3′ ends are self-complementary, bringing a fluorophore and a quencher into close proximity. Fluorescence is restored when the molecular beacon binds to a complementary target (e.g., ss-DNA), allowing the detection of unlabeled oligonucleotides. The use of "molecular beacons" in solution has proven to be a useful fluorescent method with a high stability, selectivity, and specificity, compared with similar assays performed using single-stranded DNA.[21] Situma et al. reported that the hybridization using molecular beacons as a probe immobilized on the surface was much more specific than that in bulk solution.[22] DNA hairpins, functionalized at one end with fluorescent[23,24] or electroactive labels[25−28] and then immobilized onto solid substrates, have been utilized to develop useful sensors for the selective detection of oligonucleotides. Du et al.[23] developed fluorescent biosensors for the detection of *Staphylococcus aureus femA* and *mecR* methicillin-resistant genes by the immobilization of hairpin DNA (loop 21, 30-mer, stem 9 × 2) stem-loop labeled with tetramethylrhodamine on a gold substrate that served as a more efficient quenching agent with a detection limit of 10 nM. They[24] also designed single-spot multianalyte molecular beacon biosensors using rhodamine and Cy5 as reporters. Heeger et al. developed electrochemical DNA sensors by immobilizing hairpin DNA (loop 17-mer, stem 5 × 2) labeled with an electroactive reporter (ferrocene carboxylic acid) on a gold electrode for the determination of 17-mer target DNA with concentrations as low as 10 pM[25] and single-stranded unpurified PCR amplicons produced from as few as 90 gene copies.[26] On hybridization with complementary target ss-DNA, the distance between the label and the surface of the electrode was significantly altered, leading to a large, readily measurable electrochemical signal change. Jin et al.[27] reported an electrochemical DNA sensor for the highly selective detection of the p53 gene with a detection limit of 0.2 nM by immobilizing hairpin DNA (loop 15-mer, stem 5 × 2) on a gold electrode and using methylene blue as an external redox indicator. To the best of our knowledge, ECL DNA biosensors using hairpin DNA as a recognition element have not been reported.

The aim of the present work is to develop a highly selective ECL biosensor using hairpin DNA as a recognition element. A schematic diagram of the ECL DNA biosensor based on a hairpin-DNA probe tagged with ruthenium complex is shown in Figure 1. An ECL probe, thiolated hairpin DNA tagged with ruthenium complex, is self-assembled on the surface of a gold electrode. In the absence of target ss-DNA, the hairpin DNA is in the folded configuration in which its termini are held in close proximity to the surface of the electrode, allowing the generation of a strong ECL signal. Upon hybridization with a target ss-DNA, the stem-loop of the hairpin DNA is converted into a linear double helix, removing the ruthenium complex tag from the electrode surface, thus resulting in the decrease of the ECL signal. In this paper, an ECL biosensor for the detection of DNA hybridization using hairpin DNA as a recognition element was fabricated and characterized. The effect of different loop lengths of the hairpin DNA on the selectivity of the ECL biosensor has been discussed.

EXPERIMENTAL SECTION

Materials. Ruthenium(III) chloride hydrate was purchased from ACROS Organics (Japan). *N*-hydroxysuccinimide (NHS), 2,2′-bipyridyl-4,4′-dicarboxylic acid (dcbpy), *N*,*N*′-dicyclohexyl carbodiimide (DCC), and sodium hexafluorophosphate were purchased from Sigma (U.S.A.). Tripropylamine (TPA), 2,2′-bipyridine, and mercaptohexanol were obtained from First Reagent Corporation of Shanghai (China). All reagents were of analytical grade, and Millipore Milli-Q water (18 ΩM) was used throughout. A concentration of 10 mM phosphate buffer saline (PBS, pH 7.40, 0.10 M NaCl + 10 mM KH_2PO_4/K_2HPO_4) was used as hybridization buffer and washing solution. The hairpin DNA H1 and its target were adopted from ref 29, while the hairpin DNA H2 and H3 and their target were designed according to ref 23 (as shown in Table 1). All DNA oligonucleotides were acquired from SBS Genetech. Co., Ltd. (China).

(20) Tyagi, S.; Kramer, F. R. *Nat. Biotechnol.* **1996**, *14*, 303−308.
(21) (a) Bonnet, G.; Krichevsky, O.; Libchaber, A. *Proc. Natl. Acad. Sci. U.S.A.* **1998**, *95*, 8602−8606. (b) Bonnet, G.; Tyagi, S.; Libchaber, A.; Kramer, F. R. *Proc. Natl. Acad. Sci. U.S.A.* **1999**, *96*, 6171−6176.
(22) (a) Situma, C.; Moehring, A. J.; Noor, M. A. F.; Soper, S. A. *Anal. Biochem.* **2007**, *363*, 35−45. (b) Situma, C.; Hashimoto, M.; Soper, S.A. *Biomol. Eng.* **2006**, *23*, 213−231.
(23) Du, H.; Strohsahl, C. M.; Camera, J.; Miller, B. L.; Krauss, T. D. *J. Am. Chem. Soc.* **2005**, *127*, 7932−7940.
(24) Strohsahl, C. M.; Du, H.; Miller, B. L.; Krauss, T. D. *Talanta* **2005**, *67*, 479−485.
(25) Fan, C. H.; Plaxco, K. W.; Heeger, A. J. *Proc. Natl. Acad. Sci. U.S.A.* **2003**, *100*, 9134−9137.
(26) Lai, R. Y.; Lagally, E. T.; Lee, S. H.; Soh, H. T.; Plaxco, K. W.; Heeger, A. J. *Proc. Natl. Acad. Sci. U.S.A.* **2006**, *103*, 4017−4021.
(27) Jin, Y.; Yao, X.; Liu, Q.; Li, J. H. *Biosens. Bioelectron.* **2006**, *22*, 1126−1130.
(28) Miranda-Castro, R.; de-los-Santos-Álvarez, P.; Jesús Lobo-Castañón, M.; Miranda-Ordieres, A. J.; Tuñón-Blanco, P. *Anal. Chem.* **2007**, *79*, 4050−4055.
(29) Steichen, M.; Buess-Herman, C. *Electrochem. Commun.* **2005**, *7*, 416−420.

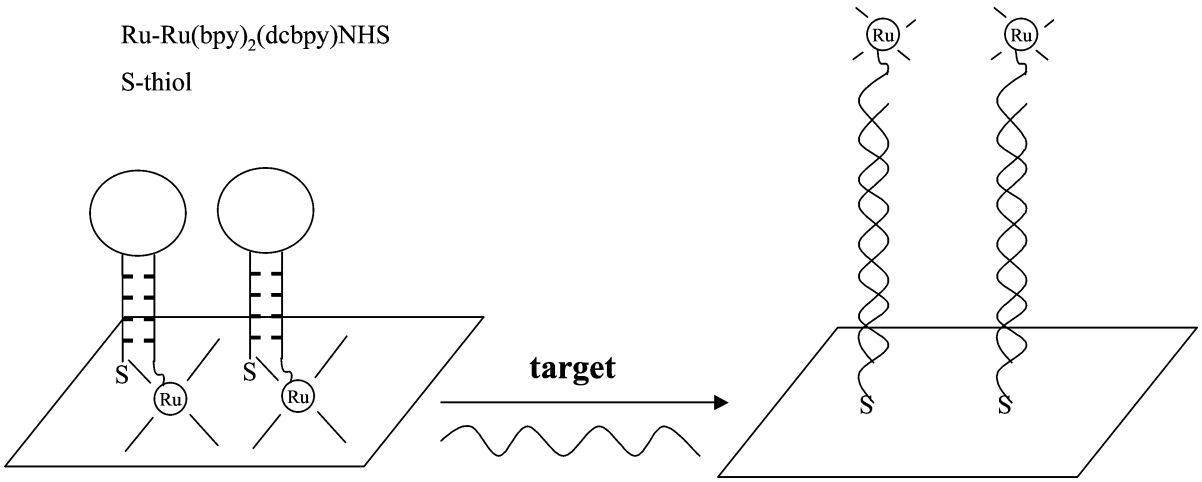

Figure 1. Schematic diagram of the hairpin-DNA probe detection for DNA hybridization.

Table 1. DNA Hairpin Probes and Their Targets

name	sequence
H1	5′-SH-$(CH_2)_6$-GTGAGC**CAAGACGGAAAGACCC**GCTCAC-$(CH_2)_6$-NH_2-3′, loop 16, bases, stem 6 × 2
H2	5′-SH-$(CH_2)_6$-GTGAGC**AACACCTTCTACACCTCCATA**GCTCAC-$(CH_2)_6$-NH_2-3′, loop 21, bases, stem 6 × 2
H3	5′-SH-$(CH_2)_6$-GTGAGC**TCATAACCTTCAGCAAGCTTTAACTCATAG**GCTCAC-$(CH_2)_6$-NH_2-3′, loop 30, bases, stem 6 × 2
T1 (H1 complement)	5′-GGGTCTTTCCGTCTTG-3′ (16 bases)
T2 (H2 complement)	5′-TATGGAGGTGTAGAAGGTGTT-3′ (21 bases)
T3 (H3 complement)	5′-CTATGAGTTAAAGCTTGCTGAAGGTTATGA-3′ (30 bases)
T1M1 (single mismatch of H1)	5′-GGGTCTTTGCGTCTTG-3′ (16 bases)
NT1(noncomplementary of H1)	5′-CAGGAAACAGCTATGA-3′ (16 bases)

Apparatus. The experimental setup for ECL measurements consisted of a CHI 600B workstation (Shanghai Chenhua Instruments, Shanghai, China) and an ultraweak chemiluminescence analyzer controlled by a personal computer with the BPCL program (Institute of Biophysics, Chinese Academy of Sciences, Beijing, China). A commercial cylindroid glass cell was used as an ECL cell. A three-electrode system composed of a biosensor or a disk gold electrode (diameter = 1.5 mm) as working electrode, a platinum plate as counter electrode, and a Ag/AgCl (saturated KCl) as reference electrode. For detecting ECL, the cell was placed directly in front of a photomultiplier (PMT, operated at −900 V) and the PMT window was only opened toward the working electrode to eliminate the blank CL and the ECL from the counter electrode.[30] The UV−vis spectrum was recorded using a UV−vis spectrophotometer (TU-1900, Beijing Puxi, China).

Synthesis of ECL Probes. Ruthenium bis(2,2′-bipyridine)-(2,2′-bipyridine-4,4′-dicarboxylic acid)-*N*-hydroxysuccinimide ester ([Ru(bpy)$_2$(dcbpy)NHS]) was synthesized according to previously published protocols.[31−33] The ECL probe P1, Ru(bpy)$_2$(dcbpy)-NHS-H1 (abbreviated as P1), was synthesized according to ref 34 with slight modifications as needed (see more details in the Supporting Information). The synthesis of Ru(bpy)$_2$(dcbpy)NHS-H2 (abbreviated as P2) and Ru(bpy)$_2$(dcbpy)NHS-H3 (abbreviated as P3) was achieved following the same protocol used for P1 except that H2 or H3 replaced H1.

Fabrication of ECL Biosensors. The gold electrode was pretreated by mechanically polishing with 0.3 μm Al_2O_3, ultrasonicated in water for 3 min, subsequently electrochemically cleaned by a linearly scanning potential between +0.2 and +1.5 V in 0.10 M H_2SO_4 and finally rinsed with water. The cleaned electrode was immersed in 200 μL of the above-synthesized ECL probe solution with a desired concentration and incubated for an appropriate time at 37 °C to immobilize the ECL probe on the surface of the electrode. The resulting electrode was thoroughly rinsed with 10 mM PBS to remove the unbound ECL probe on the surface of the electrode, immersed in 0.10 M PBS (pH 7.40, 0.10 M NaCl + 0.10 M KH_2PO_4/ K_2HPO_4) containing 1.0 mM mercaptohexanol for 1 h to block the uncovered surface of the electrode, and finally rinsed thoroughly with water.[35] The ECL biosensor obtained was stored in 0.10 M PBS in the dark.

ECL Measurements. The ECL biosensor was immersed in 200 μL of 10 mM PBS containing different concentrations of target DNA for 30 min at 37 °C, followed by a thorough washing with 10 mM PBS to remove unbound target DNA. The ECL measurement was performed at a constant potential of +0.85 V in 2.0 mL of 0.10 M PBS containing 0.10 M TPA. The concentration of target DNA was quantified by a decrease of ECL peak height ΔI ($\Delta I = I_0 - I$), where I_0 is the ECL peak height before hybridization and I is the ECL peak height after hybridization.

(30) Qi, H. L; Zhang, C. X. *Anal. Chim. Acta* **2004**, *501*, 31−35.
(31) Terpetschnig, E.; Szmacinski, H.; Malak, H.; Lakowicz, J. R. *Biophys. J.* **1995**, *68*, 342−350.
(32) Shimdzu, T.; Iyoda, T.; Izaki, K. *J. Phys. Chem.* **1985**, *89*, 642−645.
(33) Kalyanasundaram, K.; Nazeeruddin, Md. K.; Grätzel, M.; Viscardi, G.; Savarino, P.; Barni, E. *Inorg. Chim. Acta* **1992**, *198−200*, 831−839.
(34) URL: http://www.probes.com/media/pis/mp00143.pdf.
(35) Tyagi, S.; Bratu, D.; Kramer, F. R. *Nat. Biotechnol.* **1998**, *16*, 49−53.

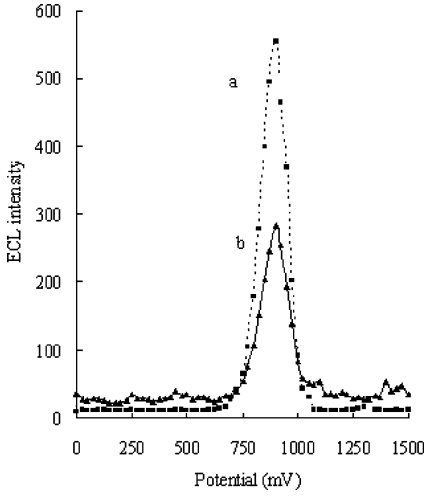

Figure 2. The ECL−potential profiles of $Ru(bpy)_2(dcbpy)NHS$ and P1 with a scan rate of 50 mV s^{-1} in 0.10 M PBS containing 0.10 M TPA. Curve a (■), 3.8×10^{-8} M $Ru(bpy)_2(dcbpy)NHS$; curve b (▲), 8.5×10^{-8} M P1.

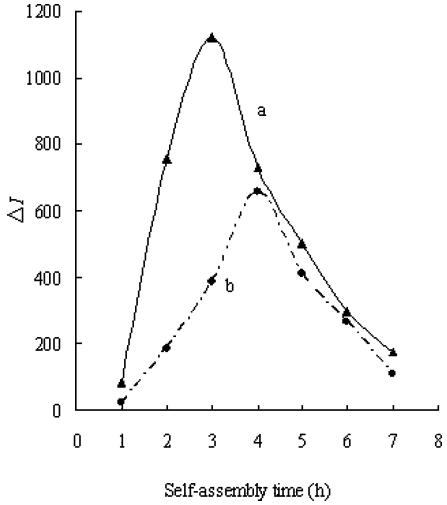

Figure 3. Effect of self-assembly time of P1 on ΔI. Curve a (▲) 8.5×10^{-6} M P1; 4.0×10^{-8} M T1. Curve b (◆) 8.5×10^{-8} M P1; 4.0×10^{-9} M T1. Hybridization time was 30 min. ECL measurements are performed in 0.10 M PBS containing 0.10 M TPA. The applied potential was 0.85 V.

RESULTS AND DISCUSSION

Characterization of the ECL Probes. The ECL probe (P1) synthesized was characterized by UV−vis spectroscopy (UV−vis absorption spectra of hairpin DNA H1, $Ru(bpy)_2(dcbpy)NHS$, and ECL probe P1 are shown in Figure S-1, Supporting Information). The results indicate that the $Ru(bpy)_2(dcbpy)NHS$ tag has been attached to H1. The concentrations of $Ru(bpy)_2(dcbpy)NHS$ synthesized and the ECL probes were estimated, on the basis of UV absorbance at 457 nm, to be 5.84×10^{-2} M $Ru(bpy)_2(dcbpy)$-NHS, 8.5×10^{-5} M P1, 5.8×10^{-5} M P2, and 5.5×10^{-5} M P3, respectively.

The ECL probe (P1) was also characterized by the ECL method in 0.10 M PBS containing 0.10 M TPA at a gold electrode using a linear potential scan technique. Figure 2 shows ECL intensity-potential profiles of $Ru(bpy)_2(dcbpy)NHS$ (curve a) and P1 (curve b). From Figure 2, it can be seen that both ECL peaks appear at near +900 mV, which is close to that (+950 mV) in ref 13, indicating that the ECL behavior of P1 is similar to that of $Ru(bpy)_2(dcbpy)NHS$ and $Ru(bpy)_2(dcbpy)NHS$ is attached to ss-DNA. The ECL intensity of $Ru(bpy)_2(dcbpy)NHS$ was nearly 4-fold higher than that of ECL probe P1 at the same concentration. This indicates that the ECL efficiency of ECL probe P1 decreases, which may be deduced by the fact that the diffusion coefficient of P1 decreases due to the increase of the molecular weight of P1.

Optimization of Self-Assembly Time. In ECL biosensor design, the immobilization of an ECL probe consisting of a molecular recognition element and an ECL signal-producing compound on the surface of a transducer plays an important role because the working potential and sensitivity are dependent upon these factors. Here, the ECL probe P1 was immobilized on the surface of a gold electrode through a self-assembled process. It was found that the ECL response of the DNA biosensor was strongly affected by the probe density of the ECL probe on electrode, which is related to the self-assembly time of the probe onto the gold electrode and the concentration of the ECL probe used. Therefore, the self-assembly time was optimized at two concentrations of the ECL probe P1. Figure 3 shows the effect of self-assembly time on the decreased ECL intensity (ΔI) at two different concentrations of P1. From Figure 3 curve a, it can be seen that ΔI increases with increasing self-assembly time from 1 to 3 h and reaches a maximum at 3 h. This is attributed to the fact that the probe density increases from 6.6×10^{11} to 8.8×10^{11} (8.5×10^{-6} M P1) molecules cm^{-2}. The surface density of hairpin DNA immobilized on the surface of the gold electrode at two concentrations of the ECL probe P1 was characterized by chronocoulometry in 10 mM Tris−HCl containing 50 mM $[Ru(NH_3)_6]^{3+}$ according to the method employed previously.[36] With further increase in the self-assembling time, however, ΔI decreased, attributed to steric and electrostatic hindrance arising from the more tightly packed probe and some interstitial space between the probes, which are necessary for high hybridization efficiency. Similar phenomena were also reported for the immobilization of DNA on a gold surface.[23] From Figure 3 curve b, it can be seen that ΔI increased with increasing self-assembly time from 1 to 4 h and reached a maximum at 4 h. This was also attributed to the fact that the probe density increases from 1.2×10^{11} (1 h) to 5.8×10^{11} (3 h) and to 6.7×10^{11} (4 h) molecules cm^{-2}. Comparing curve a with curve b in Figure 3, ΔI in curve b was lower than that in curve a at the same time. This was attributed to the fact that the ECL background of the sensors fabricated with higher P1 concentration was higher than that with lower P1 concentration. We concluded that the optimum self-assembly time should be chosen for different concentrations. Therefore, the self-assembly time of 3 h was employed for high concentrations of P1, and a period of 4 h was utilized for low concentrations of P1 to obtain a high sensitivity from the ECL biosensors.

Optimization of Test Conditions. Important experimental parameters including applied potential and hybridization time for the ECL biosensors were optimized. The influence of the applied constant potential on the ECL intensity of the biosensor using P1 was examined, and the results are shown in Figure 4. From Figure

(36) Steel, A. B.; Herne, T. M.; Tarlov, M. J. *Anal. Chem.* **1998**, *70*, 4670−4677.

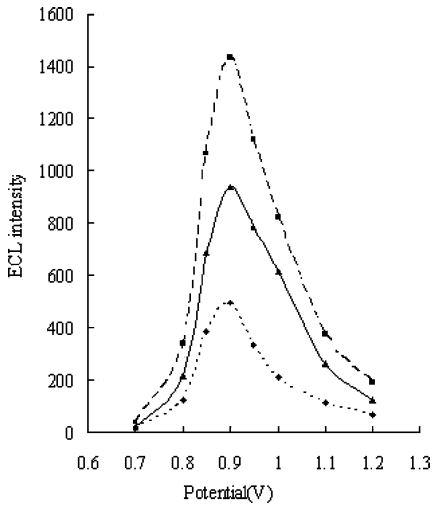

Figure 4. Effect of applied potential on ECL intensity in 0.10 M PBS containing 0.10 M TPA, 8.5×10^{-6} M P1, and 1.0×10^{-8} M T1. Key: (■) before hybridization, (◆) after hybridization, and (▲) ΔI. The self-assembly time was 3 h, and the hybridization time was 30 min.

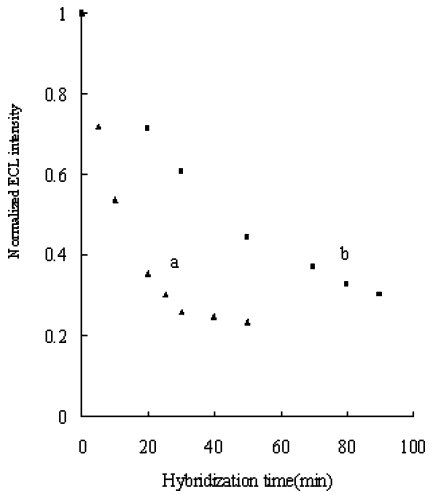

Figure 5. Effect of hybridization time on normalized ECL intensity. Curve a (▲), 8.5×10^{-6} M P1; 4.0×10^{-8} M T1. Curve b (■) 5.5×10^{-6} M P3; 4.0×10^{-8} M T3. Self-assembly time was 3 h. ECL conditions are the same as those in Figure 3.

4, it can be seen that ΔI (curve ▲) increases with the applied potential increasing from +0.7 to +0.9 V and reaches the maximum at about +0.9 V, attributed to increasing number of excited-state molecules produced during an electrochemically initiated reaction. With a further increase of the applied potential, however, ΔI decreases, attributed to the oxidative deadsorption of thiol.[37] Therefore, a constant potential of 0.85 V was chosen in the following experiments to obtain a high sensitivity and good reproducibility.

The hybridization kinetics of the ECL biosensors is dependent on not only the concentration but also the loop length and the structures of both DNA probe and target ss-DNA. Therefore, the hybridization time was optimized using two ECL biosensors by P1 (loop 16-mer, stem 6 × 2) and P3 (loop 30-mer, stem 6 × 2) for their complementary target ss-DNA T1 and T3, respectively. Figure 5 shows the dependence of the ECL signals at normalized intensity on hybridization time. From Figure 5, it can be seen that the ECL signals decrease sharply with an increase of the hybridization time. A 50% decrease was observed in the approximately 10 min after hybridization, and a steady state was reached in less than 30 min for P1−T1 (curve a). This suggests that the initial hybridization reaction proceeded quickly and the hybridization reaction was completed in about 30 min. The P3−T3 reached its steady state in about 90 min (curve b), which was much longer than that observed for P1−T1.

H1 (calculated $\Delta G_{25} = -4.7$ kcal/mol, $\Delta G_{37} = -3.1$ kcal/mol, measured $T = 60.5$ °C) has a one loop, while H3 (calculated $\Delta G_{25} = -5.2$ kcal/mol, $\Delta G_{37} = -2.1$ kcal/mol, measured $T = 51.0$ °C) has one loop at 37 °C but has three loops at 25 °C[38] (as shown in Figure S-2 in the Supporting Information). From T values and changes of Gibbs free energy at 25 °C, we can predicate that H3 is more stable than H1. However, from changes of Gibbs free energy at 37 °C, it is anticipated that H1 is more stable than H3. It is difficult to explain the results obtained using the predicated thermodynamic consideration. We attributed the longer hybridization time between H3 and T3 to the observation that H3 transfers its conformation from three loops to one loop from 25 to 37 °C. Also, it has been shown that the presence of secondary structure of the target decreases the hybridization rate. T3 (calculated $\Delta G_{37} = -0.9$ kcal/mol) is predicted to form a more stable multiple (three) loop structure than T1, which is predicted to form a one loop structure, which is consistent with the kinetic data. Steric hindrance could also account for the differences in hybridization kinetics between H1−T1 and H3−T3. H3 has 14 more nucleotides than H1 and thus potentially needs more "space" for duplex formation.[23] This idea was also demonstrated by Peterson et al.[39] and Du et. al.[23] Peterson et al.[39] investigated the surface hybridization kinetics of linear DNA for different lengths and different surface densities. It was found that longer DNA targets significantly retarded duplex formation due to steric crowding. Additionally, the faster hybridization kinetic for H1−T1 could also partially result from the slightly higher concentration of T1 used in the experiment (8.5 μM for T1 vs 5.5 μM for T3). Therefore, the hybridization time of 30 min for P1 was employed in the following experiments.

ECL Response of the Biosensors to the Complementary Target DNA. The quantitative behavior of the ECL biosensors was assessed by measuring the dependence of the decreased ECL intensity (ΔI) upon the concentration of complementary target DNA. To estimate the sensitivity of the ECL biosensors, two biosensors were fabricated using 8.5×10^{-6} M P1 for 3 h and 8.5×10^{-8} M P1 for 4 h. Under the optimized test conditions, the linear range and detection limit of two sensors to the complementary target DNA (T1) were measured. The results showed that the decreased ECL intensity (ΔI) of the biosensor (8.5×10^{-6} M P1) was logarithmically related to the concentration of T1 in the range from 5.4×10^{-8} to 5.4×10^{-6} M. The regression equation was $\Delta I = 189 \log C_{\text{ss-DNA}} + 2691$ with a regression coefficient of 0.9939. The decreased ECL intensity of the biosensors (8.5×10^{-8} M P1) was logarithmically related to the

(37) Bertolinoa, C.; MacSweeneyb, M.; Tobinb, J.; O'Neillb, B.; Sheehanb, M. M.; Colucciaa, S.; Berneyc, H. *Biosens. Bioelectron.* **2005**, *21*, 565−573.
(38) SantaLucia, J., Jr. *Proc. Natl. Acad. Sci. U.S.A.* **1998**, *95*, 1460−1465.
(39) (a) Peterson, A. W.; Wolf, L. K.; Georgiadis, R. M. *J. Am. Chem. Soc.* **2002**, *124*, 14601−14607. (b) Peterson, A. W.; Heaton, R. J.; Georgiadis, R. M. *Nucleic Acids Res.* **2001**, *29*, 5163−5168.

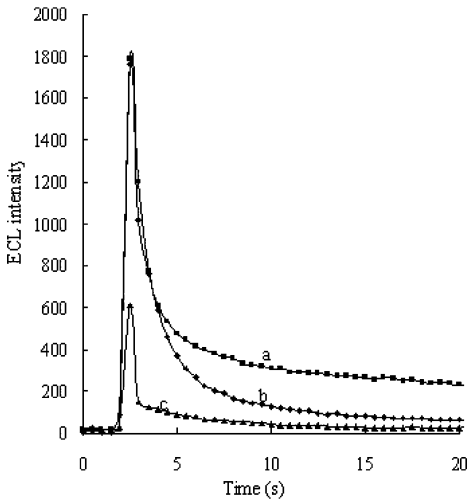

Figure 6. Comparison of hybridization events of 8.5×10^{-6} M P1 with different target ss-DNA. Key: Curve a (■), blank; curve b (◆), 4.0×10^{-6} M NT1; curve c (▲), 4.0×10^{-8} M T1. The self-assembly time was 3 h, and the hybridization time was 30 min. The ECL conditions are the same as those in Figure 3.

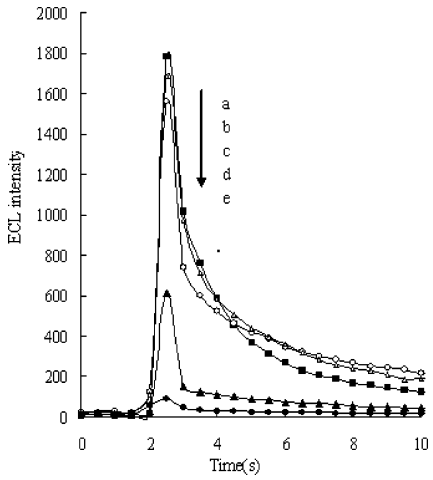

Figure 7. Kinetic response of 8.5×10^{-6} M P1 to different targets. Curve a (■), blank. Curve b (△), single-base mismatch sequence (T1M1): 4.0×10^{-8} M. Curve c (○), single-base mismatch sequence (T1M1): 4.0×10^{-6} M. Curve d (▲), complementary sequence (T1): 4.0×10^{-8} M. Curve e (●), complementary sequence (T1): 4.0×10^{-6} M. Hybridization conditions and ECL conditions are the same as those in Figure 6.

concentration of T1 in the range from 2.7×10^{-10} to 4.0×10^{-9} M. The regression equation was $\Delta I = 281 \log C$ss-DNA + 2696 with a regression coefficient of 0.9967. In the range from 4.0×10^{-9} to 5.4×10^{-8} M, the regression equation was $\Delta I = 839 \log C$ss-DNA + 7369 with a regression coefficient of 0.9952. The detection limit was 9×10^{-11} M. The detection limit is much lower than that obtained by electrochemical approaches (0.2 and 0.34 nM)[27,28] and by fluorescent approach (10 nM).[23] The relative standard derivation for the 1.0×10^{-9} M complementary sequence was 3.9% ($n = 7$).

Specificity of the ECL Biosensors. To evaluate the specificity of the ECL biosensor, one of the sensors assembled with P1 for complementary target ss-DNA (T1) was investigated and another one was done for noncomplementary target one (NT1). Figure 6 shows the ECL response of the ECL biosensor for T1 and NT1 under optimized conditions. From Figure 6 curve a, it can be seen that the ECL peak of the biosensor in the absence of target ss-DNA was significantly higher, attributed to the fact that P1 is nearly the same as that without hybridization, which was ascribed to no change of P1 formation. Comparing peak c with peak b in Figure 6, the ratio of ECL intensity decreased was 65% for 4.0×10^{-8} M complementary target DNA while the ECL intensity-decreased ratio was 1.3% for a 100-fold higher level of noncomplementary target DNA (4.0×10^{-6} M). These results are consistent with what one would predict using *RNA Structure,* version 4.5[40] (see Figure S-3 in the Supporting Information), that is, duplex formation free energy between duplex H1T1 (−22.0 kcal/mol) is much lower than that in H1−NT1 (−4.7 kcal/mol). This indicates that the ECL biosensor can be use to discriminate complementary target ss-DNA from noncomplementary target ss-DNA.

The ability to discriminate the complementary from single-base mismatch DNA is the gold standard of DNA biosensors, and the ability to sensitively detect single-base mutation is crucial to gene detection in early stage diagnosis.[27] To assess single-base mismatch discrimination, the ECL response of the sensor using P1 to single-base mismatch target DNA (T1M1), where a G−G mismatch compared with the complementary DNA (T1) was monitored after 30 min hybridization, respectively. The kinetic responses are shown in Figure 7. From Figure 7, it can be seen that the ECL intensity-decreased ratio is 5.5% for 4.0×10^{-8} M single-base mismatch target DNA, 12% for 4.0×10^{-6} M single-base mismatch target DNA, 65% for 4.0×10^{-8} M complementary target DNA, and 95% for 4.0×10^{-6} M complementary target DNA. A 8−12-fold (65%/5.5%−95%/12%) in the decrease of ECL intensity for the single mismatched target compared with the perfect match observed in our experiment is higher than that observed (2.8−12 fold) in fluorescence chips.[23] Signal mismatch discrimination with DNA probes immobilized on gold nanoparticles has been reported previously with a 4−25-fold difference in signal between the complementary and mismatch.[41−43] Our signal mismatch results are consistent with that predicted with *RNA Structure*, version 4.5 (seen Figure S-3 in the Supporting Information). The difference of binding energy for a duplex between H1−T1 (−22.0 kcal/mol, 37 °C) and H1−T1M1 (−19.6 kcal/mol, 37 °C) is 2.4 kcal/mol. Thermal melting data show that single mismatched targets form a duplex with a melting temperature 4.9 °C lower than the perfect matched duplex. Thus, the increased stability of the duplex for the perfect match relative to the single-base mismatch would translate into more efficient hybridization and thus a stronger signal. This result indicates that the ECL biosensors have potential use for the detection of single-base mismatch DNA. The specificity of hairpin DNA was, therefore, evident.

The length of the hybridization sequence, GC contents, the location of mismatch bases in the sequence, and the hybridization

(40) Mathews, D. H.; Sabina, J.; Zuker, M.; Turner, D. H. *J. Mol. Biol*. **1999**, *288*, 911−940.

(41) Dubertret, B.; Calame, M.; Libchaber, A. J. *Nat. Biotechnol*. **2001**, *19*, 365−370.

(42) Taton, T. A.; Mirkin, C. A.; Letsinger, R. L. *Science*. **2000**, *289*, 1757−1760.

(43) Storhoff, J. J.; Elghanian, R.; Mucic, R. C.; Mirkin, C. A. *J. Am. Chem. Soc*. **1998**, *120*, 1959−1964.

Table 2. Hybridization Specificity of P1, P2, and P3

ECL probe/ combine bases[f]	target DNA/ bases	ΔG (kcal/mol)[e] (37 °C)	ECL peak height	$\Delta I/I_0$ (%)
P1/16[a]−6[b]	No		1785 ± 70	0
	T1/16[c]	−22.0	612 ± 25	65
	T1M1/16[c] (15[d])	−19.6	1686 ± 65	5.5
	NT1/16[c] (3[d])	−4.7	1761 ± 61	1.3
P2/21[a]−6[b]	No		1406 ± 53	0
	T2/21[c]	−25.5	413 ± 16	71
	T3/30[c] (11[d])	−11.0	852 ± 35	39
P3/30[a]−6[b]	No		937 ± 37	0
	T3/30[c]	−35.9	324 ± 13	65
	T2/21[c] (9[d])	−7.9	713 ± 29	24

[a] The numbers in parentheses are the numbers of loop bases. [b] The numbers in parentheses are the numbers of length bases. [c] The numbers in parentheses are the numbers of bases. [d] The numbers in parentheses are the numbers of complementary bases. [e] ΔG means the free energy of duplex formation. [f] P2, P3: 2.9×10^{-6} M; T2, T3, 1.0×10^{-8} M. P1: 8.5×10^{-6} M; NT1, 4.0×10^{-6} M; M1T1, T1, 4.0×10^{-8} M.

temperature all have strong effects on duplex stability.[27,44] Therefore, the effect of different loop length of hairpin DNA on the specificity of the ECL biosensors was investigated using two ECL biosensors fabricated by the ECL probes (P2 or P3, 2.9×10^{-6} M) for two targets (T2 and T3). One of the sensors of P2 was incubated in 1.0×10^{-8} M T2 and another one was done in 1.0×10^{-8} M T3. The experiment and free energy of duplex formation predicted with *RNA Structure*, version 4.5, are shown in Table 2. From Table 2, it can be seen that the ECL peak height of the biosensor without hybridization decreases with the increase of the bases of the ECL probe. This can be attributed to the observation that the ECL efficiency decreases with the increase of the base numbers of the ECL probe. The ECL peak height of the sensor of P2 is 1406 for nonhybridization, and the decreased ratio of ECL intensity was 71% for the hybridization with T2 (21 pairs) and 39% for the hybridization with T3 (11 pairs). This suggests that the hybridization efficiency of complementary target DNA is much higher than that of the mismatched one due to the loop stem. One of the sensors of P3 was incubated in 1.0×10^{-8} M T3, and another sensor of P3 was incubated in 1.0×10^{-8} M T2. The decreased ECL intensity of P3 is 937 for nonhybridization, and the decreased ratio of ECL intensity was 65% for the hybridization with T3 (30 pairs) and 24% for the hybridization with T2 (9 pairs). The ECL intensity of different probes before hybridization decreased with increasing length of the probe, attributed to steric hindrance. The decreased ratio of the ECL intensity of P2−T2 was higher than that of P3−T3. This is attributed to fact that P2 has nine more bases than P3 and thus maybe needs more "space" for duplex formation. Additionally, the higher decreased ratio of ECL intensity for P1−T1 than that of P2−T2 and P3−T3 could also partially result from the slightly higher concentration of P1−T1 (8.5 μM for P1, 2.9 μM for P2 and P3). Our experiment results for the effect of different loop lengths of hairpin DNA on the specificity of the ECL biosensors are consistent with that predicted with *RNA Structure*, version 4.5. It is concluded that the specificity of the biosensor is related to the different loop lengths of hairpin DNA as molecular recognition elements for a DNA hybridization assay and the high specificity of the biosensor achieved using longer loop lengths of hairpin DNA.

The reusability of the ECL sensors fabricated is critically important for the sensor applications. We tested the ability to reuse the P1 sensor by regenerating the original state thermally. After the first hybridization, the sensor was washed with 90 °C water to denature the duplex and then immersed in 10 mM PBS at room temperature to refold the probe hairpins.[23] A value of ~48% of the decrease was observed. This is higher than that (40%) observed in the florescence chip of hairpin probe self-assembled on gold thin film via thiol guoup.[23] Du et al.[23] attributed the decrease in response to loss of the probe molecules from the chip surface during heating and rinsing. This problem should be solved for practical applications. The reusability could be improved by generating stronger covalent bonding to the electrode[23] and employing low ionic strength.[45] Investigation of lower ionic strength and stronger covalent bonding to the electrode to enhance the reusability is in progress.

CONCLUSION

A highly selective ECL biosensor for the detection of target ss-DNA based on hairpin DNA as a recognition element and ruthenium complex as the signal-producing compound has been designed. The hairpin ECL biosensor presents relatively sensitive DNA detection and good selectivity for discriminating complementary target ss-DNA from both noncomplementary and single-base mismatch ss-DNA. This work has demonstrated that the selectivity of ECL-based on the base-pair principle could be improved by using hairpin DNA as a recognition element. It was found that binding strength and sensitivity are dependent on the number of the matched bases. Changes in the length of the probe loop present a promising alternative approach for improvement of the sensitivity and selectivity of DNA hybridization assays. It appears that relatively longer length loops may benefit the selectivity and sensitivity of ECL-based biosensors for the detection of complementary target DNA.

ACKNOWLEDGMENT

Financial support from the National Science Foundation of China (Nos. 20775046 and 90607016,) is gratefully acknowledged.

SUPPORTING INFORMATION AVAILABLE

Synthesis and characterization of $Ru(bpy)_2(dcbpy)NHS$ (Figure S-1); secondary structure predictions of hairpins and their targets (Figure S-2); and secondary structure predictions of possible duplexes formed between hairpins and their targets (Figure S-3), as noted in text. This material is available free of charge via the Internet at http://pubs.acs.org.

(44) Ricci, F.; Lai, R. Y.; Heeger, A. J.; Plaxco, K. W.; Sumner, J. J. *Langmuir* **2007**, *23*, 6827−6834.

(45) Lubin, A. A.; Lai, R. Y.; Baker, B. R.; Heeger, A. J.; Plaxco, K. W. *Anal. Chem.* **2006**, *78*, 5671−5677.

Received for review September 21, 2007. Accepted February 9, 2008.

AC701995G